

Quantum critical behavior in the insulating region of the two-dimensional metal-insulator transition

D. J. W. Geldart^{1,2,3} and D. Neilson^{1,2,4}¹*Dipartimento di Fisica, Università di Camerino, I-62032 Camerino, Italy*²*School of Physics, University of New South Wales, Sydney 2052, Australia*³*Department of Physics and Atmospheric Science, Dalhousie University, Halifax, Nova Scotia, Canada B3H3J5*⁴*NEST CNR-INFM, I-56126 Pisa, Italy*

(Received 1 September 2007; published 13 November 2007)

We show that the quantum critical point associated with the metal-insulator transition phenomenon in two dimensions controls an extended critical region encompassing not only the usual quantum critical sector but also a range of the low-temperature insulator region. The extended range of criticality permits a unified analysis of data from the insulating region and quantum critical sector, allowing us to determine both the dynamical critical exponent z and the correlation length critical exponent ν from published data from a single experiment in the insulator critical region. We show that the critical exponents determined from the insulator sector consistently describe the temperature dependence of the resistance data from the same experiment in the quantum critical sector. This provides evidence for the presence of a quantum critical point in these systems.

DOI: [10.1103/PhysRevB.76.193304](https://doi.org/10.1103/PhysRevB.76.193304)

PACS number(s): 73.43.Nq, 71.10.Ca, 71.30.+h

Quantum phase transitions, which occur by tuning an external parameter at zero temperature, have sparked a great deal of attention recently.¹⁻³ Cases where static disorder plays an important role are particularly interesting. This Brief Report focuses on the metal-insulator (MI) transition phenomena in two dimensions in the case where the disorder is due to purely potential scattering. The tuning parameter is the carrier density n . As n is decreased at low temperature (T), a bifurcation is observed in the T -dependent resistivity $\rho(T)$ into regions with metal-like and insulatorlike slopes. This occurs at a critical density n_c and critical resistivity ρ_c .⁴⁻⁹

An analysis of experimental results for the resistivity of Si and GaAs two-dimensional (2D) semiconductor metal-oxide-semiconductor field-effect transistor and heterostructures in the vicinity of the observed separatrix is suggestive of a quantum phase transition. However, the issue of whether the metallic curves remain metallic or ultimately become insulating at very low T is difficult to establish definitively. This is partly due to the fact that the separatrix from which the critical variation of $\rho(T)$ with T should be measured is not expected to be independent of T . Thus, an apparent upturn of a metallic curve at low T may instead be an indication of a separatrix which tilts upward. The fundamental question of whether a 2D system of electrons in the absence of spin-dependent scattering or magnetic fields has a metallic phase in the low- T limit and, therefore, a critical point in the phase diagram still has no definitive answer.

Theoretical work on MI transition phenomena in two dimensions has been carried on at two levels. First principles calculations of properties of weakly disordered electron systems have been made by perturbative renormalization group (RG) methods. An important achievement of the RG has been the prediction that a metallic phase can be stabilized by electron-electron interactions.^{10,11} However, the low order perturbative RG results strictly apply only in the weak disorder limit where $\rho(T)$, in units of h/e^2 , is small compared to unity. In contrast, the bifurcation which signals the putative

MI transition is observed, where $\rho(T) \sim 1$ is not small. This strongly disordered regime is outside the range of low order RG perturbation theory but is amenable to phenomenological scaling arguments. In particular, it has been shown that scaling theory accounts for the separatrix at the critical density and for the MI transition phenomenon observed in its immediate vicinity.^{9,12}

In this Brief Report, we apply phenomenological scaling arguments to develop a strategy to interpret experimental data and to test for the existence of a quantum critical point (QCP). Assuming the observed MI transition phenomena to be due to a continuous quantum phase transition, consider the generic features of the phase diagram in the temperature and density plane proposed in Fig. 1. The semiline $n > n_c$ at $T=0$ corresponds to the metallic limit of a conducting state with disorder. The semiline $n < n_c$ at $T=0$ is the ground state insulating limit. The point ($T=0, n=n_c$) is the QCP of the transition. In the neighborhood of the QCP, where both T and $\delta_n=(n-n_c)/n_c$ are both small, physical properties will exhibit criticality.

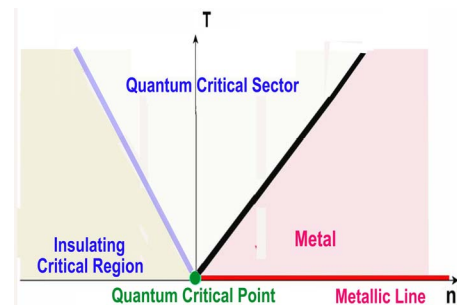


FIG. 1. (Color online) Generic phase diagram with a QCP at a critical density n_c separating insulating and metallic phases at $T=0$. For a finite range of nonzero T sufficiently close to the QCP, thermal properties of both the quantum critical sector and the insulating critical sector are determined by the critical exponents of the QCP.

In terms of scaling theory, we are assuming that the QCP is a scale invariant repulsive fixed point and that $n-n_c$ is the leading relevant perturbation. At $T=0$, $n-n_c$ determines the correlation length scale $\xi \sim |\delta_n|^{-\nu}$ in the vicinity of the MI transition. At finite T , another length scale is relevant, the thermal length $L_T \sim 1/T^{1/z}$, where z is the dynamical critical exponent. A critical behavior occurs when ξ and L_T are both much larger than microscopic length scales of the system. At $n=n_c$ or for any $L_T \ll \xi$, the thermal length determines the rate of decay of correlations. This is the usual quantum critical (QC) sector.¹⁻³

In addition, the region of the phase diagram on the insulating side of the transition, which is sufficiently close to the QCP and has $L_T \gg \xi$, must also exhibit criticality since both ξ and L_T are large. We refer to this neighborhood of the QCP as the insulating critical (IC) region. It is well established that critical exponents in the QC sector are determined by the QCP.^{1-3,9} However, for the same reasons, the part of the insulator which is sufficiently close to the QCP will have its scaling properties determined by the exponents of the QCP. The fact that the regions of the insulator near the QCP and the QC sector share the same critical exponents will cease to be true only if another fixed point becomes dominant as the RG flow proceeds in the insulator at even lower T .

Critical properties on the metallic side of the transition, $n-n_c > 0$, also reflect the influence of the QCP, but an additional feature contributes. On the metallic line, there is a continuum of gapless electron-hole excitations. These soft modes cause correlation functions to be nonanalytic in the $T=0$ limit.^{13,14} This nonanalyticity is a general feature of both pure and disordered many-fermion systems.³ In effect, the soft electron-hole excitations cause generic scale invariance along the entire metallic line. The overall critical behavior in the low- T limit near the MI transition for $n-n_c > 0$ is thus determined by the combined effect of the QCP and the metallic line, both of which exhibit scale invariance. In this Brief Report, we focus on QC and IC sectors, so we do not need to consider any specific properties of the metallic phase.

The implications of these points are illustrated in Fig. 1. We start at fixed density with $n < n_c$ in the QC sector and reduce T . We exit the QC sector and cross over into the region of the insulating phase. The analysis of experimental resistivity data taken at points along such paths can reveal the single universal $\rho(T)$ as a function of L_T/ξ . There can be different forms for this function in the limiting cases of large and small L_T/ξ , but the critical exponents are the same, provided the path is sufficiently close to the QCP.

We next develop a scaling equation for the critical behavior of $\rho(T)$ in the IC region. Scaling equations for the resistance can be expressed in the form $d\rho/dx = f(\gamma_{ee}, \rho)$, where $x = \log L$, with L as the length of the system or the thermal length L_T . The γ_{ee} symbolically indicates dependence on the e - e scattering amplitudes as additional variables.

The critical resistance ρ_c is obtained as the limiting value of ρ in the large L_T limit when the density is fixed at $n=n_c$. In simplified scaling pictures, this dependence is neglected and the separatrix is identified as the curve for which $d\rho(T)/dT = 0$. However, this does not give the correct $n=n_c$ since γ_{ee} varies with the renormalization rescaling of L_T . This causes

the bifurcation ‘‘point’’ to vary smoothly with T , so there is no unique relation between the sign of $\rho - \rho_c$ and the sign of $n - n_c$ and the separatrix is ‘‘tilted.’’ We will show below how the effect of the tilted separatrix can be accounted for empirically. After isolating this effect, the experimental data can be described by scaling equations of the simpler form $d\rho/dx = f(\rho)$.

The dominant variation of ρ with L is expected to be exponential in the insulating limit, $\rho \propto \exp(L/\xi)$, with ξ as the correlation length. In order to determine the prefactor of the exponential, we require an explicit scaling equation. We take $d\rho/dx$ in the insulator to be represented as a series in powers of ρ and $\log \rho$. The series is positive and monotonically increasing with ρ . The only *a priori* condition is that ρ must remain finite for all finite L and can diverge only in the limit $L \rightarrow \infty$. We denote the leading term in this series at large L by $k(\rho)^\alpha (\log \rho)^\beta$, where α , β , and k are all positive. The maximum allowed values of α and β are $\alpha = \beta = 1$ since otherwise ρ would diverge prior to the $L \rightarrow \infty$ limit. The solution of the scaling equation at large L , $d\rho/dx = k\rho \log \rho$, is then $\log \rho \sim L^k$. Taking the leading variation of ρ to be exponential in L fixes $k=1$. Equivalently, ρ has a log-normal probability distribution in the strong disorder limit.

The prefactor of the leading exponential factor is obtained by including subleading corrections in the scaling equation, $(1/\rho)d\rho/dx = \log \rho - a - b/\log \rho + \dots$, where a and b are constants. First, neglect the series in inverse powers of $\log \rho$. The solution is then $\rho(L)/\rho_0 = \exp\{\log[\rho(L_s)/\rho_0](L/L_s)\}$, where $a = \log \rho_0$ sets the resistance scale and $\rho(L_s)$ is the resistance at an arbitrary starting point L_s . The right hand side is independent of the starting point since $\{\log[\rho(L_s)/\rho_0]\}/L_s$ is $1/\xi$.

Including the corrections in inverse powers of $\log \rho$, the explicit solution becomes $\rho(L) = \rho_0 \exp[(L/\xi) + b\xi/(2L) + \dots]$. To describe the resistance at finite T , we replace L by the thermal length $L_T \propto 1/T^{1/z}$, where z is the dynamical critical exponent of the QCP. The temperature dependence of the resistance in the insulator is then given by

$$\rho(T) = \rho_0 [1 + c(T/T_1)^{1/z} + \dots] \exp[(T_1/T)^{1/z}]. \quad (1)$$

We see that the subleading T dependence is very weak (relative to the leading exponential), making it difficult to detect at low T . Consequently, the prefactor is essentially ρ_0 for $T \ll T_1$. Both ρ_0 and T_1 will be density dependent but are independent of T .

The scaling equation for the resistivity in the QC sector follows from the hypothesis of a QCP. After correcting for the tilted separatrix, scale invariance at the critical density implies $d\rho/dx = 0$ when $\rho = \rho_c$. Taking $d\rho/dx$ to vanish linearly in $\rho - \rho_c$ with a slope of $1/\nu$ then provides a scaling equation. Dobrosavljević *et al.*¹² have argued that an improved description is given by applying this generic argument to the vanishing of $\log(\rho/\rho_c)$ rather than of ρ/ρ_c . In this case, each L is raised to the power of $1/\nu$. Replacing L by the thermal length L_T then gives

$$\rho(T) = \rho_c \exp\{\log[\rho(T_s)/\rho_c](T_s/T)^{1/z\nu}\}. \quad (2)$$

Equation (2) is similar to Eq. (1), but with a T dependence characterized by $1/(z\nu)$ in the QC sector while only $1/z$

appears in the IC region. Also, the resistivity scale is fixed as ρ_c in the QC sector, while the scale ρ_0 is unspecified in the IC region.

If $\log(\rho(T_s)/\rho_c)$ is further approximated by $\delta\rho/\rho_c \approx -c\delta_n$, this gives $\rho(T) = \rho_c \exp[-c\delta_n/T^{1/z\nu}]$.¹² When the density and electric field dependence is analyzed at a fixed low T , the corresponding relation is $\rho(E) = \rho_c \exp[-c'\delta_n/E^{1/(z+1)\nu}]$. Thus, from data in the QC sector alone, two separate experiments were required to determine z and ν .

We now show that both z and ν can be obtained in a single experiment on $\rho(T, n)$ in the IC region. Experimental results for the resistivity in the low- T insulating regime have been reported for a variety of 2D systems.^{7,15–20} To compare theory and experiment, we chose to analyze data for a Si sample from Ref. 17. This contains T -dependent resistivity data for both the IC region and the QC sector.

To allow for a tilted separatrix in the data, we start by identifying the two curves that span the bifurcation. In Ref. 17, the $n_- = 0.9554 \times 10^{11} \text{ cm}^{-2}$ curve exhibits a weak downturn at low T and the $n_+ = 0.9336 \times 10^{11} \text{ cm}^{-2}$ curve exhibits an upturn. For the T dependence of the separatrix, we assume a functional form $\rho_{sep}(T) = \rho_c \exp[m_{sep}T]$ since the n_- and n_+ curves are linear on a $\log \rho$ versus T plot at higher T . We fit these two curves at higher T to straight lines, with ρ_c and m_{sep} being the fitting parameters. We define the separatrix as the average of these two curves, weighted by the deviations of the straight lines from the actual T -dependent curves. Extrapolating this average to $T=0$, we deduce a critical resistivity $\rho_c = 3.757 (h/e^2)$ with a critical density $n_c = 0.9481 \times 10^{11} \text{ cm}^{-2}$, and a value for $m_{sep} = -0.1608 \text{ K}^{-1}$. Figure 2(a) shows the tilted separatrix as the solid straight line in the QC sector. In fitting to the scaling equations, we first divide all the experimental data points by this $\rho_{sep}(T)$ to eliminate the effect of the separatrix tilt.

For the insulating range of ρ , we fitted the resulting data points to

$$\rho(T) = \rho_0(n) \exp\left\{[T_0(n)/T]^{1/z}\right\}. \quad (3)$$

Equation (3) is the same as Eq. (1), with the weakly T -dependent prefactor replaced by $\rho_0(n)$ and with T_1 replaced by $T_0(n)$. To ensure that fitted data lie well inside the IC region, we selected low T , high $\rho(T)$ points by restricting $\rho(T) > \rho_{cut} = 20$. Numerical least squares methods determined a value of z for each of the curves in this region. To test consistency with respect to the range of fit, the procedure was repeated for different values of ρ_{cut} up to $\rho_{cut} = 30$. An analysis of the resulting set of values of z gave a mean value and standard deviation of $z = 2.05 \pm 0.10$. The curves in the IC region for $\rho(T) > 20$ in Fig. 2(a) show Eq. (3) for this value of z .

We now demonstrate that the critical exponent ν can also be determined from data in the IC region. Taking $z = 2.05$ to be fixed, the least squares fits of all the IC data were made into Eq. (3) to obtain $T_0(n)$ for each density curve. The fits to the data are shown in Fig. 2(a). The $T_0(n)$ are shown as the triangle points in Fig. 2(b). Since $[T_0(n)/T]^{1/z} = L_T/\xi$ in Eq. (3), it follows that $T_0(n)$ should vary as $|\delta_n|^{z\nu}$. Figure 2(b) confirms this dependence. The solid line is the best fit of

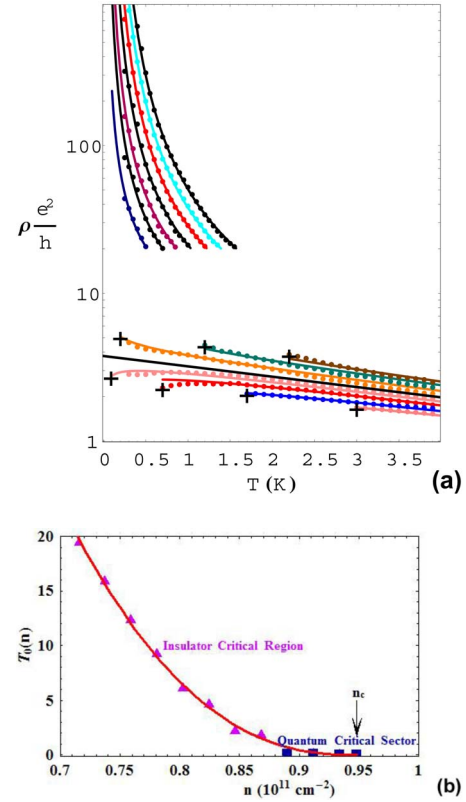


FIG. 2. (Color online) (a) Data points taken from Ref. 17. Points in the IC region are for densities (in units of 10^{11} cm^{-2}) from 0.7156 (top) to 0.8464. The cutoff is set at $\rho_{cut} = 20$ (in units of h/e^2). All points shown are in the IC region. Solid lines for these points are best fits using Eq. (3) with z and the density dependent $T_0(n)$ as the fitting parameters. In the QC sector, the data points are for densities from 0.8900 (top) to 1.0426. Solid lines for these points show Eq. (2) using the value $z\nu = 2.4$ determined from the IC region and with $\rho_c = 3.757$ determined from the separatrix (solid straight line). QC sector curves terminate when the ratio $L_T/\xi = [c|\delta_n|/T^{1/z\nu}]^\nu$ exceeds $1/3$. (b) Triangle points are our best fit values from Eq. (3) of $T_0(n) = T_1(n)$ for the data from Ref. 17 lying in the IC region. The solid line is the function $d(-\delta_n)^{z\nu}$. Rectangle points show $T_0(n) = [\rho(T_s)/\rho_c]^{z\nu} T_s$ for the Ref. 17 data in the QC sector [see Eq. (2)].

$[d(-\delta_n)]^{z\nu}$ to the triangles, with $z = 2.05$ fixed. The best fitting parameters are $d = 14.9$ and $\nu = 1.17$. Repeating this fitting, with z fixed at 1.95 and 2.15, yields $\nu = 1.20$ and $\nu = 1.15$, respectively. Thus, data from the IC region can determine *both* critical exponents of the QCP. The corresponding value of $z\nu$ is 2.4 ± 0.1 . The quality of the fits of Eq. (3) to the data in the IC region is very good, as seen in Fig. 2(b). All the data points shown satisfy $L_T/\xi > 3$.

We want to compare Eq. (1) with the predictions of the variable range hopping (VRH) theory. These theories are explicit models of conduction in the hopping regime, but they were not developed to describe a MI transition. We recall that VRH models lead to an expression^{21,22} $\rho(T) = \rho_0(T) \exp[(T_0/T)^p]$. When Coulomb interactions are included,²² the exponent p is predicted to be $p = 1/2$.

The VRH exponential T dependence agrees with experiment.^{7,15,16,18–20} However, the VRH prefactor $\rho_0(T)$ has a power law temperature dependence,^{23,24} in disagreement with experiment. The experimentally observed prefactor in the insulator at low T is T independent, as is predicted by our scaling equation [Eq. (1)]. This is a direct consequence of the scaling description of the MI transition in terms of a QCP.

We now show that the critical exponents determined from the IC region also describe the QC sector. Taking the value $z\nu=2.4$ determined from the IC region and with ρ_c determined from the separatrix, Eq. (2) then defines a $\rho(T)$ for the QC region with no free fitting parameters. Figure 2(a) shows that this predicted $\rho(T)$ is consistent with all the data points from Ref. 17 lying within the QC region, defined by $L_T/\xi = [\rho(T_s)/\rho_c]^\nu(T_s/T)^{1/z} < 1/3$. The good agreement is a confirmation (i) that z and ν can both be determined from a single experiment and (ii) that the values of z and ν obtained from the IC region are consistent with the $z\nu$ for the QC sector. This supports our premise that both regions are controlled by the QCP.

The temperature scale $T_0(n)$ for the QC sector can also be deduced. The rectangle points in Fig. 2(b) give $T_0(n) = [\rho(T_s)/\rho_c]^{z\nu} T_s$ for the $\rho(T)$ data points from Ref. 17 for $n < n_c$ in the QC sector. These rectangle points lie on the same solid line as the triangle data, confirming that the two regions have the same correlation length critical exponent. This is further evidence that the QC sector and the IC region for this finite range of T are both critical and controlled by the QCP.

The critical exponents z and ν have previously been determined only from the QC sector by an analysis of two separate experiments on density-temperature and density–electric field data.⁹ In this way, no consistency check can be obtained for the values of z and ν . Values of z range between 0.8 and 1.2, and those of ν between 1.5 and 1.9. The major source of the discrepancies with our values is the assumption made previously that the separatrix is not tilted. This can lead to an incorrect identification of the critical density, and the critical exponents depend sensitively on this choice of n_c . This emphasizes the importance of the consistency check comparing the values obtained in the IC region and the QC sector.

In summary, we have presented a scaling picture of the MI transition based on the phase diagram in Fig. 1. The QCP controls two regions of criticality, the QC sector and the IC region sufficiently close to the QCP at finite T . Hence, these two regimes share the same critical exponents z and ν . As a result, it becomes possible to unify the analysis of transport data for the QC sector and the IC regime and to obtain the critical exponent ν of the correlation length and the dynamical critical exponent z of the thermal length from a single experiment. A quantitative comparison with published experimental results (Ref. 17) shows that values of z and ν in the IC region and the QC sector are consistent. This gives support for the existence of a QCP in the 2D electron transport.

-
- ¹S. L. Sondhi, S. M. Girvin, J. P. Carini, and D. Shahar, *Rev. Mod. Phys.* **69**, 315 (1997).
- ²S. Sachdev, *Quantum Phase Transitions* (Cambridge University Press, Cambridge, 1999).
- ³D. Belitz, T. R. Kirkpatrick, and Thomas Vojta, *Rev. Mod. Phys.* **77**, 579 (2005).
- ⁴S. V. Kravchenko, W. E. Mason, G. E. Bowker, J. E. Furneaux, V. M. Pudalov, and M. D’Iorio, *Phys. Rev. B* **51**, 7038 (1995).
- ⁵S. V. Kravchenko, D. Simonian, M. P. Sarachik, W. Mason, and J. E. Furneaux, *Phys. Rev. Lett.* **77**, 4938 (1996).
- ⁶D. Simonian, S. V. Kravchenko, M. P. Sarachik, and V. M. Pudalov, *Phys. Rev. Lett.* **79**, 2304 (1997).
- ⁷P. T. Coleridge, R. L. Williams, Y. Feng, and P. Zawadzki, *Phys. Rev. B* **56**, R12764 (1997).
- ⁸M. Y. Simmons, A. R. Hamilton, M. Pepper, E. H. Linfield, P. D. Rose, D. A. Ritchie, A. K. Savchenko, and T. G. Griffiths, *Phys. Rev. Lett.* **80**, 1292 (1998); Y. Y. Proskuryakov, A. K. Savchenko, S. S. Safonov, M. Pepper, M. Y. Simmons, D. A. Ritchie, A. G. Pogosov, and Z. D. Kvon, *Phys. Status Solidi B* **230**, 89 (2002).
- ⁹E. Abrahams, S. V. Kravchenko, and M. P. Sarachik, *Rev. Mod. Phys.* **73**, 251 (2001).
- ¹⁰A. M. Finkel’stein, *Z. Phys. B: Condens. Matter* **56**, 189 (1984).
- ¹¹C. Castellani, C. Di Castro, P. A. Lee, and M. Ma, *Phys. Rev. B* **30**, 527 (1984).
- ¹²V. Dobrosavljević, E. Abrahams, E. Miranda, and S. Chakravarty, *Phys. Rev. Lett.* **79**, 455 (1997).
- ¹³D. J. W. Geldart and M. Rasolt, *Phys. Rev. B* **15**, 1523 (1977).
- ¹⁴D. Belitz, T. R. Kirkpatrick, and T. Vojta, *Phys. Rev. B* **55**, 9452 (1997).
- ¹⁵Whitney Mason, S. V. Kravchenko, G. E. Bowker, and J. E. Furneaux, *Phys. Rev. B* **52**, 7857 (1995).
- ¹⁶V. M. Pudalov, G. Brunthaler, A. Prinz, and G. Bauer, *JETP Lett.* **68**, 534 (1998).
- ¹⁷V. M. Pudalov, G. Brunthaler, A. Prinz, and G. Bauer, *JETP Lett.* **68**, 442 (1998).
- ¹⁸S. I. Khondaker, I. S. Shlimak, J. T. Nicholls, M. Pepper, and D. A. Ritchie, *Solid State Commun.* **109**, 751 (1999).
- ¹⁹S. I. Khondaker, I. S. Shlimak, J. T. Nicholls, M. Pepper, and D. A. Ritchie, *Phys. Rev. B* **59**, 4580 (1999).
- ²⁰I. Shlimak, K. J. Friedland, and S. D. Baranovskii, *Solid State Commun.* **112**, 21 (1999).
- ²¹N. F. Mott, *J. Non-Cryst. Solids* **1**, 1 (1968); M. Pollak, *Discuss. Faraday Soc.* **50**, 13 (1970); G. Srinivasan, *Phys. Rev. B* **4**, 2581 (1971).
- ²²A. L. Efros and B. I. Shklovskii, *J. Phys. C* **8**, L49 (1975).
- ²³I. L. Aleiner, D. G. Polyakov, and B. I. Shklovskii, in *Proceedings of the 22nd International Conference on Phys. Semiconductors, 1994*, edited by D. J. Lockwood (World Scientific, Singapore, 1994), p. 787 suggested that VRH without phonons [L. Fleishman, D. C. Licciardello, and P. W. Anderson, *Phys. Rev. Lett.* **40**, 1340 (1978)] might explain the T -independent prefactor, but we find the application of Fleishman *et al.*, to 2D systems still gives a power law prefactor $\propto T^{13/6}$.
- ²⁴D. N. Tsigankov and A. L. Efros, *Phys. Status Solidi B* **230**, 157 (2002); M. Pollak, *ibid.* **230**, 295 (2002).